Microchemical Journal 208 (2025) 112505

Contents lists available at ScienceDirect

Microchemical Journal

journal homepage: www.elsevier.com/locate/microc

On-line aptamer affinity solid-phase extraction capillary electrophoresis-mass spectrometry for the determination of SARS-CoV-2 nucleocapsid protein

Hiba Salim [a,1], Laura Pont [a,b,1], Estela Giménez [a], Suttinee Poolsup [c], Maxim V. Berezovski [c], Fernando Benavente [a,*]

[a] Department of Chemical Engineering and Analytical Chemistry, Institute for Research on Nutrition and Food Safety (INSA·UB), University of Barcelona, Spain
[b] Serra Húnter Program, Generalitat de Catalunya, Spain
[c] Department of Chemistry and Biomolecular Sciences, University of Ottawa, Canada

ARTICLE INFO

Keywords:
Aptamer
Capillary electrophoresis
COVID-19
In-line solid-phase extraction
Mass spectrometry
N protein

ABSTRACT

Severe acute respiratory syndrome coronavirus 2 (SARS-CoV-2) is responsible for coronavirus disease 2019 (COVID-19), which has sparked a significant global health crisis in recent years. Among its structural proteins, the nucleocapsid protein (N protein) stands out as one of the most abundant. Despite being well-recognized as an immunodominant antigen in host immune responses and a promising diagnostic biomarker, further insight into this protein with novel analytical methods is crucial for understanding the disease mechanisms. This study focuses on the development of an aptamer affinity sorbent for the purification, preconcentration, separation, characterization, and quantification of the N protein using on-line aptamer affinity solid-phase extraction capillary electrophoresis-mass spectrometry (AA-SPE-CE-MS). Microcartridges packed with a sorbent composed of magnetic bead (MB) particles modified with an aptamer against the N protein were utilized. A rigorous optimization of several method parameters resulted in the use of a lab-made hydroxypropyl cellulose (HPC)-coated capillary to prevent protein adsorption and a neutral background electrolyte (BGE) of 10 mM ammonium acetate (pH 7.0) for the separation. The sample was loaded in the BGE, and the retained protein was subsequently eluted with 1 M acetic acid (pH 2.3). The developed method demonstrated repeatability in terms of migration times and peak areas, exhibited linearity between 2.5 and 25 μg mL^{-1}, and achieved a limit of detection (LOD) of 0.5 μg mL^{-1}, providing a sensitivity enhancement of 500 times compared to CE-MS. It was finally applied to the analysis of the N protein in human saliva, pointing out its potential for establishing accurate SARS-CoV-2 complementary analytical methods.

1. Introduction

Severe acute respiratory syndrome coronavirus 2 (SARS-CoV-2) has triggered a significant surge in COVID-19 cases worldwide, leading to a global pandemic with millions of deaths [1–3]. To decrease both infection and mortality rates, the development of reliable and rapid diagnostic tools capable of detecting viral infections in their early stages is crucial. Molecular techniques such as reverse transcription-polymerase chain reaction (RT-PCR) are predominantly used for COVID-19 diagnosis [4,5], targeting the genes of specific structural proteins of the virus, including spike (S), envelope (E), and nucleocapsid (N) proteins [6]. Among them, the N protein, responsible for the packing of the SARS-CoV-2 genomic RNA, has emerged as a promising COVID-19 diagnostic biomarker, primarily due to its abundant expression during viral infection, with approximately 1,000 copies per viral particle [7–9].

While RT-PCR offers several advantages [4,5], including a wide application range, high sensitivity, and strong specificity, its complex pretreatment, lengthy processing time, and high cost have led to the emergence of serological tests, primarily relying on ELISA and lateral flow immunoassays, as the primary alternative to nucleic acid testing [10,11]. These serological tests offer notable benefits, such as affordability and ease of implementation at the point of care, facilitating the

* Corresponding author.
E-mail address: fbenavente@ub.edu (F. Benavente).
[1] Both authors contributed equally to this study.

https://doi.org/10.1016/j.microc.2024.112505
Received 13 September 2024; Received in revised form 9 December 2024; Accepted 16 December 2024
Available online 18 December 2024

massive identification of individuals previously infected by SARS-CoV-2 [10,11]. Nevertheless, their reliance on antibodies immobilized on sensing materials for non-selective detection poses a risk for the appearance of both false negatives and false positives. False negatives in antibody immunoassays can stem from multiple factors, including assay formats, the choice of viral antigens and antibody types, diagnostic testing windows, individual variability, and fluctuations in antibody levels [12,13]. Conversely, false positives frequently occur due to antibody cross-reactivity with other viruses or autoimmune diseases [12,13]. As an alternative, this work explores an innovative and direct analytical approach for the purification, preconcentration, separation, characterization, and quantification of the N protein using on-line aptamer affinity solid-phase extraction capillary electrophoresis-mass spectrometry (AA-SPE-CE-MS), an approach we previously described for the analysis of α-synuclein (α-syn) in blood [14,15], as well as concanavalin A (Con A) [16] and β-lactoglobulin (β-LG) [17] in food matrices. In this valve-free AA-SPE-CE-MS setup, a microcartridge with an AA sorbent against the protein of interest is integrated near the inlet of the separation capillary, operating in a unidirectional configuration [18,19]. This enables loading a large sample volume (typically ~50–100 μL) for selective clean-up and preconcentration, followed by injection of a small eluent volume (typically ~25–50 nL) for subsequent electrophoretic separation and selective detection by MS [18,19].

By combining the advantages of using AA-SPE sorbents and MS detection, AA-SPE-CE-MS has the potential to overcome specific limitations of the techniques currently employed for COVID-19 diagnosis while providing further insight into protein biomarkers crucial for understanding the disease mechanisms. In this sense, aptamers, which are single-stranded RNA or DNA oligonucleotides typically consisting of fewer than 100 nucleotides, present several benefits over antibodies. Aptamers are usually selected through SELEX (Systematic Evolution of Ligands by EXponential enrichment), a method involving the screening of large combinatorial libraries of oligonucleotides [20,21]. Once their sequence is established, they can be chemically synthesized at a low cost in an automated, rapid, and reproducible manner, bypassing challenges associated with antibody production, such as dependence on animals or cells and batch-to-batch variability [22]. Furthermore, aptamers offer robustness, thermal stability, tolerance to wide ranges of pH and salt concentrations, and the possibility to be chemically modified for controlled immobilization [19,22]. Several studies have described the development of aptasensors aiming to enhance sensitivity and accuracy in the detection of the N protein [7,9,23–25]. However, these efforts are hindered by the need for multistep sample preparation and, especially, the lack of molecular mass (M_r) confirmation. In contrast, the use of on-line MS detection, as in the presented AA-SPE-CE-MS method, enables a reliable identification of the target compound, thereby reducing the risks associated with false positives, false negatives, or inaccurate quantifications.

In this work, an AA-SPE-CE-MS method was developed for the analysis of the N protein using SPE microcartridges packed with magnetic bead (MB) particles modified with an appropriate aptamer. The chosen aptamer, tNSP3, was previously selected for the N protein by SELEX and characterized using other tecniques by Poolsup et al. [7]. A rigorous optimization of several AA-SPE-CE-MS method conditions, such as sample loading, washing, and eluent composition, was necessary, as well as using lab-made hydroxypropyl cellulose (HPC)-coated capillaries to prevent protein adsorption. These adjustments were crucial due to the distinct properties of the N protein, particularly its M_r and isoelectric point (pI), in comparison to the proteins analyzed by AA-SPE-CE-MS in our previous studies [14–17]. After developing an appropriate procedure for sample clean-up to prevent microcartridge saturation, the AA-SPE-CE-MS method proved to be effective in analyzing the N protein in human saliva, underscoring its potential for establishing accurate complementary analytical methods for COVID-19 research.

2. Experimental section

2.1. Chemicals

All buffers and solutions were prepared with analytical reagent-grade chemicals, unless otherwise indicated. Acetic acid (HAc, glacial, 100 %), ammonium hydroxide (25 % (v/v)), ammonium acetate (NH_4Ac, ≥99.9 %), formic acid (HFor, 99.0 %), hydrochloric acid (37 % (v/v)), potassium chloride (99.0 %), potassium dihydrogen phosphate (≥99.0 %), potassium hydroxide (≥95.0 %, pellets), sodium chloride (≥99.5 %), sodium hydrogen phosphate (≥99.0 %), sodium hydroxide (≥99.0 %, pellets), LC-MS grade methanol (MeOH), hydroxypropyl cellulose (HPC, 100,000 M_r, ≥95.0 %), bovine serum albumin (BSA, ≥98 %), and Tween® 20 (≥99.0 %) were obtained from Merck (Darmstadt, Germany). LC-MS grade propan-2-ol was supplied by Scharlau (Barcelona, Spain). LC-MS grade water was provided by Fisher Scientific (Loughborough, UK). Ethanol (100 %) was supplied by Panreac AppliChem (Barcelona, Spain). The amino-modified single-stranded DNA-aptamer against the N protein (tNSP3, 5′/5AmMC6/CAGCGTCACGTGTTGTTCCCCATTGTACTGATTCGTCGTGGCAT-3′, 44-mer, M_r = 13,650) [7] was provided by Integrated DNA Technologies (Coralville, IA, USA). Commercially available activated agarose-based MBs (MAGicBeads ACT) of 45–165 μm diameter were supplied by MAGic BioProcessing (Uppsala, Sweden). Fused silica capillaries (75 and 250 μm inner diameter (i.d.) × 365 μm outer diameter (o.d.)) were obtained from Polymicro Technologies (Phoenix, AZ, USA).

2.2. Solutions and sheath liquid

For CE-MS analysis under acidic conditions, a 2 M HAc BGE (pH 2.2) was utilized, while a 10 mM NH_4Ac BGE (pH 7.0) was employed for CE-MS under neutral conditions and AA-SPE-CE-MS. Protein elution in AA-SPE-CE-MS was carried out with a 1 M HAc solution (pH 2.3). All solutions were filtered through a 0.22 μm nylon filter (Macherey-Nagel, Düren, Germany) prior to analysis. A sheath liquid composed of 60:40 (v/v) propan-2-ol:water with 0.25 % (v/v) HFor was delivered at a flow rate of 3.3 μL min^{-1} using a KD Scientific 100 series infusion pump (Holliston, MA, USA). Prior to use, the sheath liquid underwent ultrasonic degassing for 10 min.

2.3. Protein standard solutions

Recombinant SARS-CoV-2 N protein with a His-tag (M_r of 51,386), as previously described by Poolsup et al. [7], was expressed in-house using *Escherichia coli* (*E. coli*). A protein stock solution of 1,000 μg mL^{-1} was prepared in water, aliquoted, and stored in a freezer at −20 °C. Prior to analysis, low M_r excipients were removed from the stock solution by passing it through low-protein binding centrifugal filters of 30,000 M_r cut-off (MWCO) (Amicon® Ultra-0.5 centrifugal filters, Millipore, Bedford, MA, USA), following a protocol outlined in a previous study [26]. Working standard solutions were freshly prepared by diluting with proper volumes of water (for CE-MS) or the neutral BGE (for AA-SPE-CE-MS).

2.4. Saliva samples

Saliva samples were collected from a healthy donor using the SpeciMAX™ Saliva Collection Kit (Fischer Scientific) following the manufacturer's instructions. The study was approved by the Ethical and Scientific Committees of UB. A precipitation with ice-cold ethanol was used for sample clean-up prior to analysis by AA-SPE-CE-MS [27]. After centrifugation at 12,000×*g* and 4 °C for 15 min to remove food debris and cells, the resulting supernatant was spiked with the N protein stock solution to a final concentration of 25 μg·mL^{-1}. Two hundred microliters of the spiked saliva were mixed with 800 μL of ice-cold ethanol and vortexed thoroughly. The mixture was then subjected to overnight

incubation at −20 °C. Following incubation, the mixture underwent centrifugation at 15,000×*g* and 4 °C for 30 min. After that, the supernatant was discarded, and the resulting pellet was air-dried at room temperature for 30 min. Subsequently, the pellet was dissolved in 400 μL of the neutral BGE and filtered through Amicon® Ultra-0.5 30,000 MWCO centrifugal filters [26] to a final volume of 200 μL.

2.5. Preparation of the AA sorbent

The activated MBs to couple the amino-modified single-stranded DNA-aptamer were functionalized following procedures outlined in previous studies [16,17,19]. Briefly, a 200 μL aliquot of the MBs solution (20 μL of sedimented MBs) was vortexed, and the supernatant was removed by magnetic separation. The MBs were then washed three times with 200 μL of phosphate-buffered saline (PBS) containing 0.1 % (v/v) Tween 20® (PBS-T). After removing the supernatant, the resulting MBs were resuspended in the same volume of PBS-T. Following the addition of 10 μL of activation buffer to the MBs suspension, the mixture was incubated for 15 min at room temperature. The supernatant was then removed, and the MBs were washed with 200 μL of PBS-T before being resuspended in 150 μL of PBS-T. Subsequently, 50 μL of a 100 μM aptamer solution in PBS was added to the MBs suspension, and the mixture was incubated for 40 min at room temperature. Afterwards, the supernatant was removed, and the aptamer-functionalized MBs (AA-MBs) underwent three successive washes with 200 μL of PBS before being resuspended in the same volume of PBS. To block residual reactive groups on the AA-MBs, 200 μL of blocking buffer (5 % (m/v) BSA in PBS-T) was added, and the mixture was incubated for 2 h at 37 °C. Finally, the supernatant was removed, and the AA-MBs were washed three times with 200 μL of PBS. The AA-MBs were either used immediately or stored in PBS containing 20 % (v/v) ethanol at 4 °C when not in use.

2.6. CE-MS

CE-MS experiments were conducted using a 7100 CE coupled with an orthogonal G1603A sheath-flow interface to a 6220 orthogonal acceleration time-of-flight (oa-TOF) LC/MS spectrometer (Agilent Technologies, Waldbronn, Germany). Control, data acquisition, and processing for CE and TOF-MS were managed with ChemStation and MassHunter software (Agilent Technologies). Mass spectrometer settings were as follows: capillary voltage 4,000 V, drying gas temperature 300 °C, drying gas flow rate 4 L min^{-1}, nebulizer gas 7 psi, fragmentor voltage 325 V, skimmer voltage 80 V, and OCT 1 RF Vpp voltage 300 V. Data were collected in profile at 1 spectrum·s^{-1} within the range of 100–3,200 *m/z*, utilizing the high-resolution mode (4 GHz). Separations were conducted at 25 °C using a capillary with dimensions of 72 cm total length (L_T) × 75 μm i.d. × 365 μm o.d. All capillaries flushes were at 930 mbar. For CE-MS analysis under acidic conditions, new capillaries were activated by flushing with 1 M NaOH (15 min), water (15 min), and the acidic BGE (30 min). For CE-MS analysis under neutral conditions, HPC-coated capillaries were prepared to prevent protein adsorption on the inner capillary wall. The capillaries were coated as described in a previous study [28]. Briefly, a 5 % (m/v) HPC solution was prepared, sonicated, heated (1 h at 40 °C), and stirred overnight at room temperature to remove air bubbles. A 100 cm fused silica capillary was flushed sequentially with MeOH (10 min), 1 M KOH (10 min), water (10 min), 1 M HCl (10 min), and 5 % (m/v) HPC solution (1 h). N_2 was passed through the capillary at 1.5 bar using a Kitasato flask connected to an N_2 source for 60 min or until bubbles were visible at the outlet end. If clogging occurred, the outlet end was cut (0.5 cm). After 10 min of bubbling, the capillary was heated in a household oven at 140 °C for 60 min with continuous N_2 flow. After coating one end, the capillary was reversed, flushed with fresh 5 % (m/v) HPC solution (1 h), and the process was repeated for the other end. Finally, the capillary was cut to the desired length (i.e, 72 cm L_T). HPC-coated capillaries were conditioned by flushing with the neutral BGE for 15 min. With both CE-MS conditions (acidic and neutral), samples were hydrodynamically injected at 50 mbar for 10 s (around 50 nL [29]). Separation was conducted by applying a voltage of +25 kV (normal polarity, cathode in the outlet). For CE-MS under neutral conditions, a 25-mbar pressure was applied during the separation. The autosampler was maintained at 10 °C using an external water bath (Minichiller 300, Peter Huber Kaltemaschinenbau AG, Offenburg, Germany). Between runs, the capillary underwent conditioning by flushing with water (2 min) and acidic BGE (2 min) (for CE-MS under acidic conditions with fused silica capillaries) or with 1 M HAc (2 min), water (2 min), and neutral BGE (2 min) (for CE-MS under neutral conditions with HPC-coated capillaries).

2.7. AA-SPE-CE-MS

Fritless particle-packed microcartridges for unidirectional AA-SPE-CE-MS were prepared following procedures detailed in previous studies [14–17,19]. Microcartridge preparation proved to be straightforward and reproducible due to the larger average size of the sorbent particles compared to the i.d. of the separation capillary. As shown in Fig. 1, the microcartridge (0.7 cm L_T × 250 μm i.d. × 365 μm o.d. capillary) was vacuum-filled with the AA-MB-based sorbent and connected with plastic sleeves between two HPC-coated capillary fragments (7.5 cm L_T × 75 μm i.d. × 365 μm o.d. (inlet) and 52.5 cm L_T × 75 μm i.d. × 365 μm o.d. (outlet)). AA-SPE-CE-MS capillaries were conditioned under the optimized conditions by flushing with the neutral BGE for 5 min. Samples (prepared in the neutral BGE) were loaded at 930 mbar for 10 min (around 65 μL [29]), followed by a 1-min flush with the neutral BGE to eliminate non-retained molecules and fill the capillary before the electrophoretic separation and detection. To prevent contaminants from entering to the mass spectrometer during these steps, the nebulizer gas

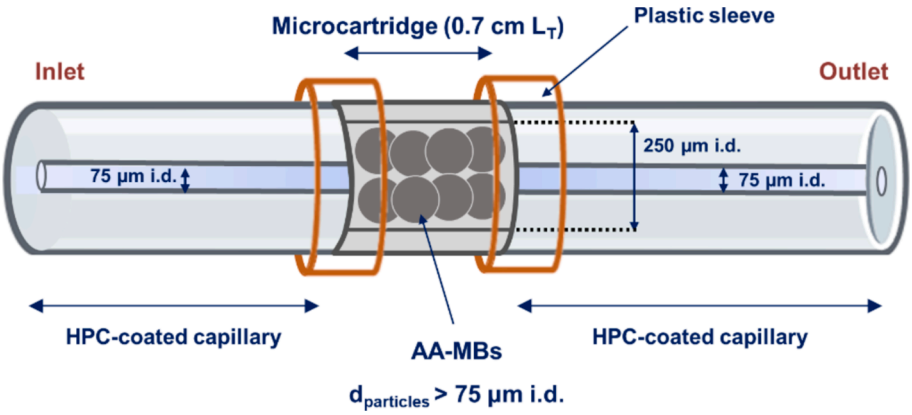

Fig. 1. Scheme of the fritless particle-packed microcartridge used for AA-SPE-CE-MS.

and the ESI capillary voltage were switched off. Subsequently, both were switched on, and a small volume of eluent consisting of 1 M HAc (pH 2.3) was injected at 50 mbar for 60 s (around 360 nL [29]). For a rapid and repeatable protein elution, the small eluent plug was pushed with the neutral BGE at 50 mbar for 100 s before applying the separation voltage (+25 kV) and a small pressure (25 mbar) to compensate for the microcartridge counter-pressure. Between runs, the capillary was flushed with water for 1 min, followed by eluent injection at 50 mbar for 1 min, and then flushed with water again for 1 min.

2.8. Quality parameters

The optimized CE-MS and AA-SPE-CE-MS methods were validated using N protein standard solutions to assess repeatability, linearity, the limit of detection (LOD), and microcartridge lifetime (in the case of AA-SPE-CE-MS). Repeatability (n = 3) was evaluated at 500 μg mL^{-1} for CE-MS (acidic and neutral conditions) and at 25 μg mL^{-1} for AA-SPE-CE-MS, calculating the percent relative standard deviation (%RSD) of migration times (t_m) and peak areas obtained from the extracted ion electropherograms (EIEs) of the N protein most abundant molecular ions (charges from +35 to +65). Linearity was determined from the limit of quantification (LOQ) to the limit of linearity (LOL), ensuring a coefficient of determination (R^2) greater than 0.99 by analyzing standard solutions in different concentration ranges (250–1,000 μg mL^{-1} for CE-MS under acidic conditions, 350–1,000 μg mL^{-1} for CE-MS under neutral conditions, and 2.5–25 μg mL^{-1} for AA-SPE-CE-MS). This set of experiments allowed the experimental estimation of the LOD, defined as the lowest concentration yielding a signal-to-noise ratio (S/N) higher than 3. The microcartridge lifetime in AA-SPE-CE-MS was finally evaluated by repeatedly analyzing an N protein standard solution at a concentration of 10 μg mL^{-1}, until peak areas in the EIEs decreased more than 25 % compared to the mean value of the first three analyses.

3. Results and discussion

3.1. CE-MS analysis: acidic conditions

In general, optimal results for intact protein analysis by CE-MS in ESI+ are achieved using acidic volatile BGEs and sheath liquids. These conditions effectively enhance protein ionization and sensitivity, as previously described for the analysis of α-syn [14,15], Con A [16], and β-LG [17] using aqueous BGEs with HAc and propan-2-ol:water sheath liquids with HFor. In this work, various acidic conditions were evaluated for the analysis of the N protein, including different BGEs (100 mM HAc pH 2.9, 1 M HAc pH 2.3, and 2 M HAc pH 2.2) combined with sheath liquids of 60:40 (v/v) propan-2-ol:water and 0.05 or 0.25 % (v/v) HFor. The highest sensitivity for the N protein analysis was achieved using a BGE of 2 M HAc (pH 2.2) and a sheath liquid of 60:40 (v/v) propan-2-ol: water with 0.25 % (v/v) HFor, as in the analysis of Con A [16] and β-LG [17]. Fig. 2-A illustrates the extracted ion electropherogram (EIE) (i), mass spectrum (ii), and deconvoluted mass spectrum (iii) obtained for the CE-MS analysis of a 1,000 μg mL^{-1} N protein standard solution under the optimized acidic conditions. As expected with a high M_r protein, the mass spectrum was very complex, presenting a wide cluster of highly overlapped multiply-charged ions (with charges from +35 to +65) (Fig. 2-A-ii). The only proteoform detected in the analyzed standard was the free N protein (M_r of 51,386), as the recombinant N protein expressed in *E. coli* was not expected to undergo post-translational modifications (PTMs) during bacterial expression. Minor peaks in the deconvoluted mass spectrum of Fig. 2-A-iii were primarily attributed to $Na^+ + K^+$ adducts [30], as previously observed in the analysis of α-syn [14,15]. Under the optimized acidic conditions, the CE-MS method demonstrated linearity within the N protein concentration range of 250–1,000 μg mL^{-1} ($R^2 > 0.99$) and the LOD was 100 μg mL^{-1}. Repeatability assessment at a concentration of 500 μg mL^{-1} yielded satisfactory %RSD values (n = 3) for both t_m and peak areas (0.2 % and 14.1 %, respectively).

3.2. CE-MS analysis: Neutral conditions

Despite the promising results obtained with acidic CE-MS conditions, we failed to detect the N protein using AA-SPE-CE-MS with an acidic BGE and a 100 mM ammonia (pH 11.2) eluent, which were the optimized conditions in previous methods for the analysis of α-syn [14,15], Con A [16], and β-LG [17]. Under these conditions, the protein retention on the AA sorbent was compatible with filling the capillary with the acidic BGE, followed by a small plug of basic pH solution for the elution, and subsequent separation and detection. At this point, upon comparing the acidic pIs of α-syn (4.7), Con A (5.4), and β-LG (4.9) [19] with the basic pI of the N protein (10.1) [31], we hypothesized that the aptamer-protein interaction was strongly influenced by the pI. Therefore, the N protein would be washed away during the washing and capillary filling steps with the acidic BGE before the elution, separation, and detection. The fact that the N protein was a larger protein than the rest (M_r = 51,386 vs 14,459 for α-syn, 25,598 for Con A, and 18,364 and 18,277 for β-LG A and B, respectively) was also probably influencing protein retention. Both effects have been previously described in the literature as potentially affecting the affinity of aptamers against proteins [32].

To address this issue, we developed an alternative CE-MS method under neutral pH conditions, utilizing 10 mM NH_4Ac pH 7.0 as a BGE (the composition of the sheath liquid remained unchanged). Initially, fused silica capillaries were employed. However, repeatability issues and broad peaks were observed due to protein adsorption to the ionized silanol groups of the inner wall of the fused silica capillary, which were negatively charged to a large extent at pH 7.0. Protein adsorption in fused silica capillaries may be particularly relevant at these pH values for large proteins, especially if the pH remains below the protein pI, and that was the case with the N protein. To prevent this phenomenon and improve CE performance, a static, permanent coating of HPC polymer was adopted [28]. This coating created a neutral hydrophilic surface on the capillary inner wall, minimizing the electroosmotic flow (EOF) and protein adsorption [28,33,34]. Fig. 2-B depicts the EIE (i), mass spectrum (ii), and deconvoluted mass spectrum (iii) obtained for the CE-MS analysis of a 1,000 μg mL^{-1} N protein standard solution under the optimized neutral conditions using an HPC-coated capillary. The results closely resembled those obtained under acidic conditions. As can be observed, the N protein appeared at a similar t_m (compare Fig. 2-A-i and Fig. 2-B-i) due to the application of a 25-mbar pressure to counterbalance the EOF suppression during the separation with HPC-coated capillaries and the lower protein global positive charge at pH 7.0. In addition, the mass spectrum (Fig. 2-B-ii) and the resulting deconvoluted mass spectrum (Fig. 2-B-iii) displayed practically identical profiles to those observed with the acidic BGE (Fig. 2-A-ii and −iii). This indicated that the charge of the detected N protein molecular ions was not affected by the increase in the pH of the BGE, even though the neutral pH remained below its pI, due to the use of the acidic pH sheath liquid. Under the optimized neutral conditions, the CE-MS method was linear within the N protein concentration range of 350–1,000 μg mL^{-1} ($R^2 >$ 0.99), the LOD was 250 μg mL^{-1} (2.5-fold higher than with acidic conditions due to the lower protein ionization efficiency at neutral pH conditions), and repeatability was similar to the acidic conditions (% RSD (n = 3) at 500 μg mL^{-1} were 0.7 % and 5.2 % for t_m and peak areas, respectively).

3.3. AA-SPE-CE-MS analysis

The AA sorbent for AA-SPE-CE-MS was prepared using the aptamer with high selectivity and affinity against the N protein (K_D in the range of 0.6–3.5 nM), as previously described by Poolsup et al. [7]. Contrary to our previous works [14–17,19], as explained before, a neutral BGE (10 mM NH_4Ac pH 7.0) was selected to avoid protein release before the elution, which, in this case, required an acidic eluent. This emphasizes

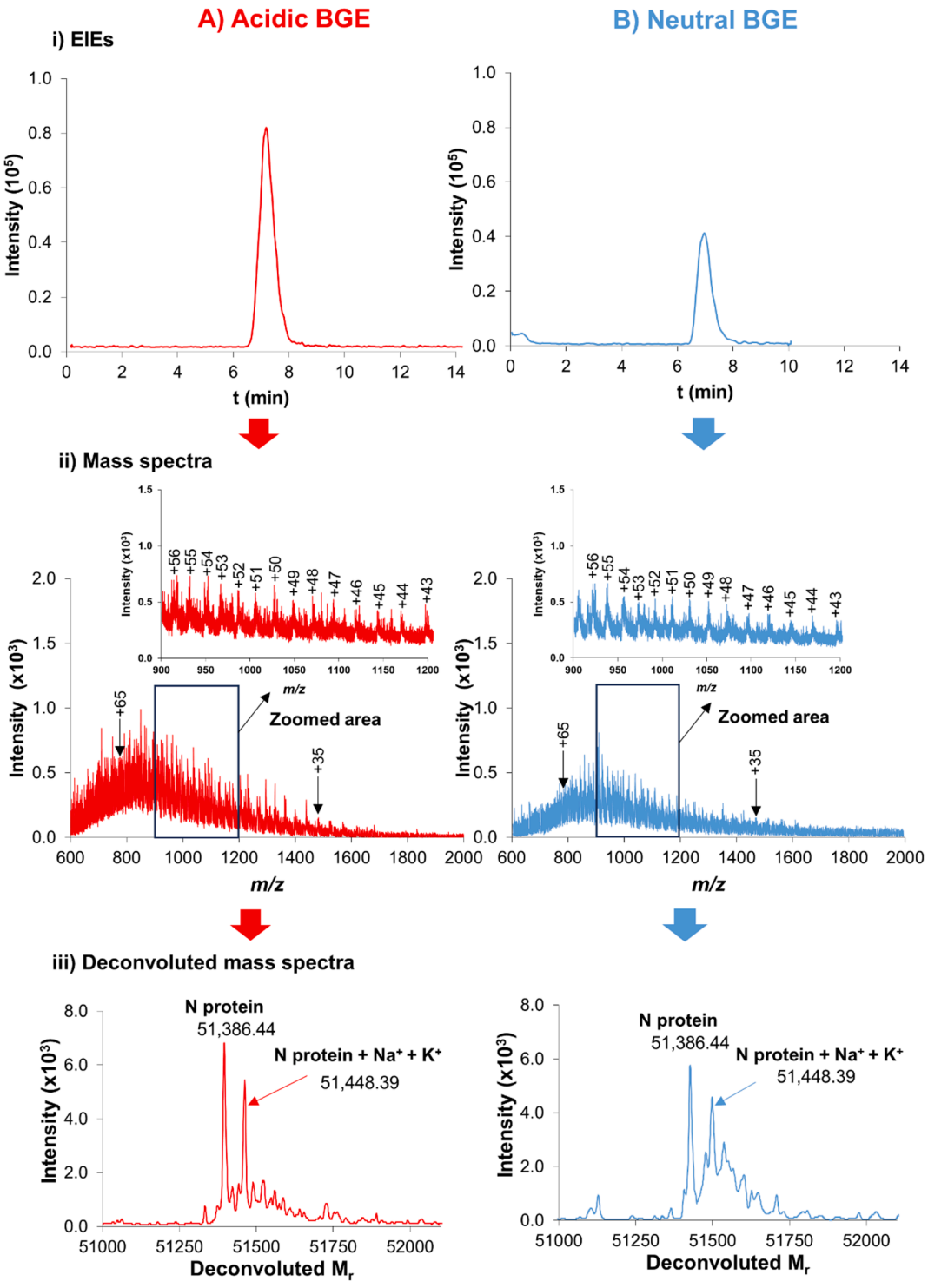

Fig. 2. (i) Extracted ion electropherograms (EIEs) (charges from +35 to +65), (ii) mass spectra, and (iii) deconvoluted mass spectra for the CE-MS analysis of a 1,000 μg mL^{-1} N protein standard solution under (A) acidic conditions using a fused silica capillary and (B) neutral conditions using an HPC-coated capillary. Typical M_r errors in the deconvolution are ~20 ppm ($E_r = (M_{r\ experimental} - M_{r\ theoretical})/M_{r\ theoretical} \times 10^6$).

the importance of carefully considering the BGE and elution conditions based on the target protein biomarker when developing AA-SPE-CE-MS methods. In terms of eluent composition, various acidic volatile eluents were tested to disrupt the aptamer-protein interaction (i.e., 100 mM HAc pH 2.9, 1 M HAc pH 2.3, and 2 M HAc pH 2.2), with 1 M HAc pH 2.3 demonstrating the highest sensitivity and repeatability in t_m and peak areas (see Supplementary Fig. S-1-A). To avoid aptamer denaturation and prolong microcartridge lifetime, concentrations higher than 2 M HAc in these aqueous eluents were not explored. The investigation into volatile eluents was expanded to test hydroorganic mixtures containing 80 % (v/v) MeOH in the presence of 1 M HAc. The findings were comparable to those achieved with the aqueous eluents (see Supplementary Fig. S-1-A). For this reason and to avoid a possible sorbent degradation during the elution caused by the organic solvents, the aqueous solution consisting of 1 M HAc pH 2.3 was chosen for subsequent experiments. The volume of the eluent plug was investigated by injecting the eluent at

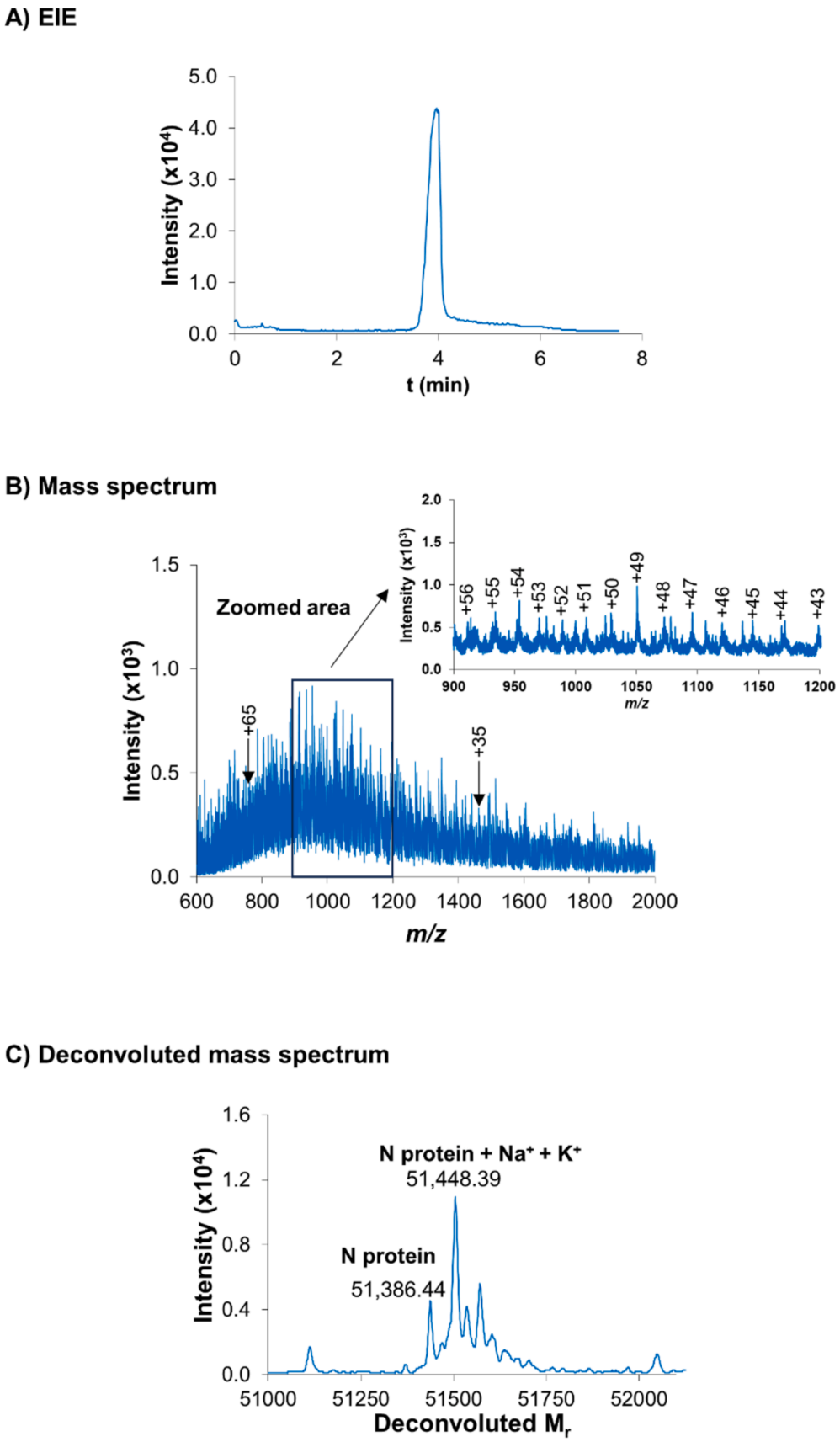

Fig. 3. (A) Extracted ion electropherogram (EIE) (charges from +35 to +65), (B) mass spectrum, and (C) deconvoluted mass spectrum for the AA-SPE-CE-MS analysis of a 25 μg mL^{-1} N protein standard under the optimized conditions. Typical E_r in the deconvolution are ~20 ppm.

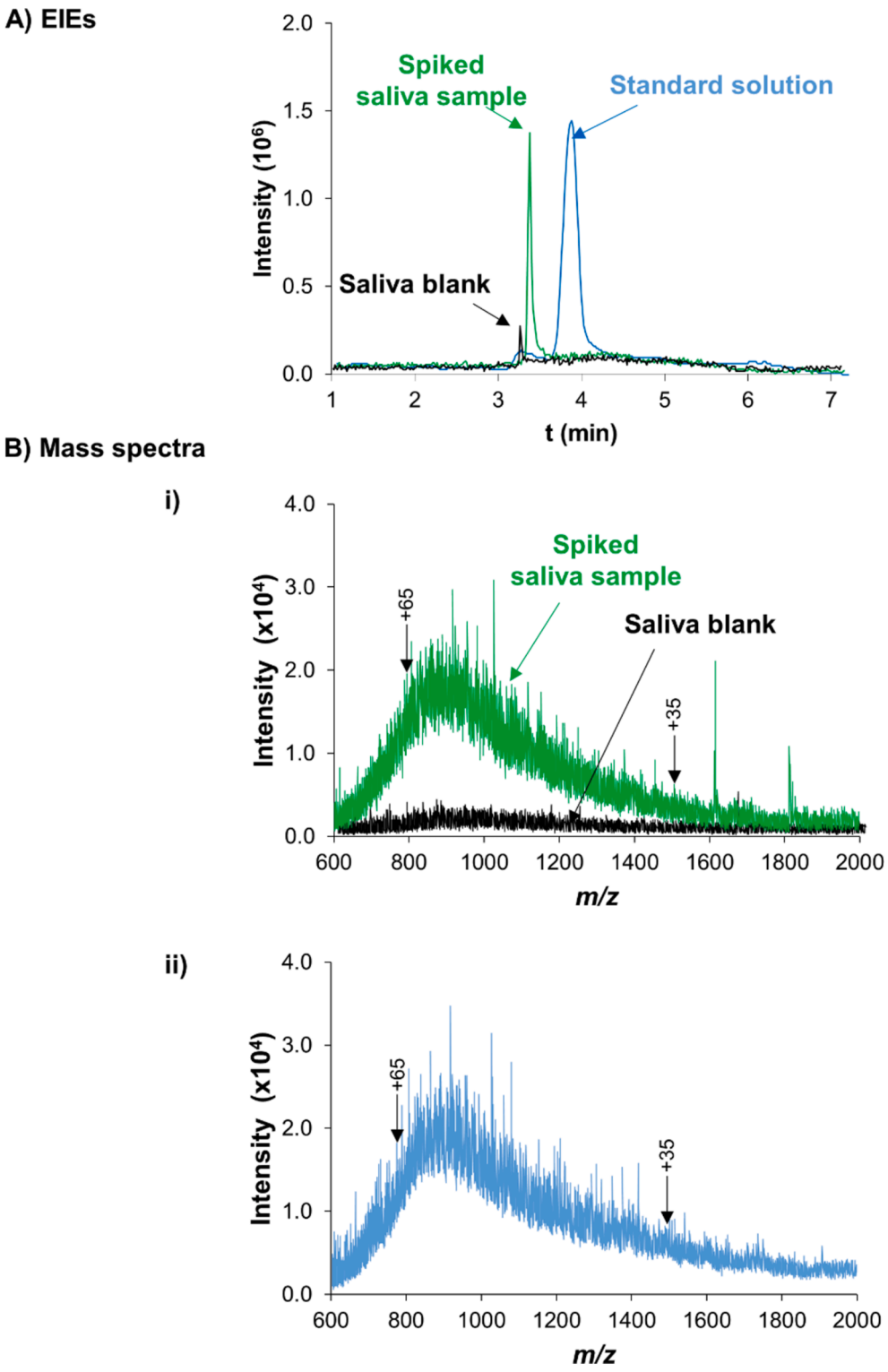

Fig. 4. (A) Extracted ion electropherograms (EIEs) (charges from +35 to +65) obtained by AA-SPE-CE-MS for the analysis of a saliva sample spiked at 25 μg mL^{-1} with N protein (green), a non-spiked saliva sample (saliva blank, black), and a 25 μg mL^{-1} N protein standard solution (blue). (B) Mass spectra obtained by AA-SPE-CE-MS for (i) a saliva sample spiked at 25 μg mL^{-1} with N protein (green) and a saliva blank (black), and (ii) a 25 μg mL^{-1} N protein standard solution (blue). Typical E_r in the deconvolution are ~20 ppm (deconvoluted mass spectra not shown). (For interpretation of the references to colour in this figure legend, the reader is referred to the web version of this article.)

50 mbar for 20, 40, and 60 s (around 120, 240, and 360 nL [29]). A higher amount of the N protein was detected when injecting the eluent at 40 and 60 s instead of 20 s, but the most repeatable results were at 60 s (see Supplementary Fig. S-1-A). Longer elution times than 60 s were discarded, as they lead to broader peaks and smaller preconcentration factors. In all these experiments, to avoid carry over, the capillary was washed between analyses with water, a small plug of eluent, and again with water. Regarding sample loading, standard solutions were prepared in the neutral BGE because lower peak areas were observed when using water or PBS. The addition of 5 mM $MgCl_2$ was also explored,

given its known potential to promote the binding between the aptamer and the protein [7]. However, the results did not improve, and samples were loaded in the neutral BGE. In subsequent experiments, the sample loading time was investigated, introducing a 25 μg mL^{-1} N protein standard solution at 930 mbar from 2.5 to 15 min. As can be observed in Supplementary Fig. S-1-B, the maximum peak area for the N protein was observed with a loading time of 10 min (around 65 μL [29]). Prolonged loading times resulted in decreased N protein peak areas as the sample breakthrough volume was exceeded, causing the protein to be washed away. Therefore, a loading time of 10 min was chosen to maximize protein recovery. Under the optimized conditions, consecutive analyses exhibited repeatability in both t_m and peak areas. At a concentration of 10 μg mL^{-1}, the %RSDs (n = 3) were 0.4 % and 6.8 %, respectively, mirroring values obtained by CE-MS. The method demonstrated satisfactory linearity ($R^2 > 0.99$) across the range of 2.5–25 μg mL^{-1}, and the microcartridges exhibited a lifetime of approximately 25 analyses. Interestingly, the LOD was 0.5 μg mL^{-1}, representing a 500-fold improvement compared to the CE-MS method. This preconcentration factor was higher than those obtained in our previous works for the analysis of α-syn, Con A, and β-LG by AA-SPE-CE-MS (500-fold vs. 100-fold for α-syn [14] and Con A [16], and 200-fold for β-LG [17]), pointing out the excellent performance of the aptamer against the N protein under the optimized conditions. Additionally, the achieved LOD (0.5 μg mL^{-1}, equivalent to around 9 nM) is comparable to the LOD previously described by Poolsup et al. for the analysis of the N protein using the same tNSP3 aptamer to establish a label-free aptamer-based biolayer interferometry method [7]. As illustrated in Fig. 3, the AA-SPE-CE-MS analysis of a 25 μg mL^{-1} N protein standard closely resembled that obtained with CE-MS under neutral conditions (Fig. 2-B). The mass spectrum revealed the broad cluster of highly overlapped multiply-charged ions (same charges, compare Fig. 2-B-ii and Fig. 3-B), while the deconvoluted mass spectrum showcased the M_r of the N protein proteoform (M_r of 51,386), with a higher intensity observed for the N protein + Na^+ + K^+ (compare Fig. 2-B-iii and Fig. 3-C) due to the specific conditions of the AA-SPE-CE-MS method.

3.4. Analysis of saliva samples

In the analysis of intact proteins within complex matrices, such as biological fluids (e.g., blood, cerebrospinal fluid, saliva, etc.), AA sorbents, as other highly selective SPE sorbents where the affinity ligand is immobilized in an inert solid support, may suffer from non-selective retention of interferents and matrix effects [18,19]. This is especially critical when working at the microscale, with microcartidges containing a limited amount of AA sorbent. Therefore, overcoming this challenge and ensuring an accurate AA extraction requires a sample clean-up before AA-SPE-CE-MS. For the analysis of the N protein in human saliva samples, different sample clean-up pretreatments were tested. Initially, a dilute and shoot procedure was evaluated, diluting the saliva samples at different ratios (1:2, 1:4, and 1:10 (v/v)) either with neutral BGE or PBS. As the N protein was not detected under these conditions, desalting with 30,000 and 50,000 MWCO centrifugal filters was also explored. However, no satisfactory results were obtained, highlighting the complexity of the sample matrix. Subsequently, a common method to remove α-amylase, the most abundant protein in human saliva, was employed by adding starch (1 g of starch per 10 mL of saliva) and then removing the resulting insoluble complex by centrifugation [35]. However, the N protein remained undetected, likely due to interactions with the starch-amylase complex, which were not disrupted even when the pH of the solution was increased to 11.0 (pH > pI of the N protein). Finally, the N protein was detected using a simple protein precipitation method. This involved precipitating saliva proteins with ice-cold ethanol, reconstituting the pellet in the neutral BGE, and desalting using 30,000 MWCO centrifugal filters. Fig. 4 displays the EIEs (A) and mass spectra (B) obtained by AA-SPE-CE-MS for a spiked saliva at 25 μg mL^{-1}, a non-spiked saliva (i.e., saliva blank), and a 25 μg mL^{-1} N protein standard solution. As depicted in the EIEs of Fig. 4-A, the N protein was only detected in the spiked saliva sample and in the standard solution. The repeatability of both t_m and peak areas in the spiked saliva sample (%RSD (n = 3) of 3.0 % and 9.6 %, respectively) was slightly lower compared to the values previously obtained with the standard solution (Section 3.3). Additionally, a minor shift in t_m, along with differences in peak area and shape compared to the standard, were observed. These variations were likely due to the complexity of the saliva matrix, even after the sample clean-up pretreatment applied. Non-specific retention of certain matrix components on the AA sorbent, followed by their subsequent elution, couldn't be ruled out. Additionally, in unidirectional AA-SPE-CE-MS, sample matrix components could modify the inner capillary wall during sample loading. Fig. 4-B-i shows the mass spectrum confirming the detection of the N protein in the spiked sample. As can be observed, the mass spectrum and deconvoluted M_r values in the spiked saliva were practically identical to those obtained for the standard solution (Fig. 4-B-ii), while the N protein was not detected in the saliva blank. The N protein could be detected until 2.5 μg mL^{-1} (around 45 nM), confirming the potential of the proposed AA-SPE-CE-MS method to directly purify, preconcentrate, separate, characterize, and quantify the N protein in saliva samples from suspected COVID-19 patients. The concentration of N protein in these samples can vary widely depending on factors such as the stage of infection, viral load, and symptom severity [36]. The achieved LODs fall within the higher range of N protein concentrations reported in saliva by various biosensors and bioassays [36,37]. However, these methods lack the ability to provide unequivocal identification and accurate quantification supported by M_r and structural information.

4. Conclusions

We developed an AA-SPE-CE-MS method for the purification, preconcentration, separation, characterization, and quantification of the SARS-CoV-2 N protein. The development of this methodology posed great challenges, particularly due to the basic pI and high M_r of the protein. In contrast to our previous works with proteins having acidic pIs and M_r ranging from around 14,500 to 25,600 (i.e., α-syn, Con A, and β-LG), a neutral BGE (10 mM NH_4Ac pH 7.0), an acidic eluent (1 M HAc pH 2.3), and a lab-made HPC-coated capillary were employed. These choices aimed to prevent protein release before the elution, and protein adsorption on the inner capillary wall during separation, underscoring the importance of carefully considering the properties of the target protein when developing AA-SPE-CE-MS methods. Under the optimized conditions with standards, microcartridge lifetime (around 25 analyses) and repeatability (0.4 and 6.8 %RSD for t_m and peak areas) were satisfactory, the method was linear between 2.5 and 25 μg mL^{-1}, and the LOD was 0.5 μg mL^{-1} (500 times lower than by CE-MS, 250 μg mL^{-1}). For the analysis of human saliva samples, we established a clean-up pretreatment involving protein precipitation with ice-cold ethanol, reconstitution of the pellet in the neutral BGE, and desalting using 30,000 MWCO centrifugal filters before AA-SPE-CE-MS. Results were satisfactory, enabling the unequivocal determination of the N protein at low levels, thereby preventing false positives and negatives often encountered in non-MS-based biosensors or bioassays. Beyond reliable diagnostics, the M_r and structural information provided by on-line MS detection in AA-SPE-CE-MS could contribute to a deeper understanding of the COVID-19 disease mechanisms and the evaluation of differential behaviors among virus variants.

CRediT authorship contribution statement

Hiba Salim: Writing – review & editing, Writing – original draft, Validation, Methodology, Investigation. **Laura Pont:** Writing – review & editing, Writing – original draft, Validation, Methodology, Investigation. **Estela Giménez:** Writing – review & editing, Supervision, Investigation, Conceptualization. **Suttinee Poolsup:** Writing – review & editing,

Methodology, Investigation. **Maxim V. Berezovski:** Writing – review & editing, Supervision, Investigation, Funding acquisition, Conceptualization. **Fernando Benavente:** Writing – review & editing, Supervision, Investigation, Funding acquisition, Conceptualization.

Declaration of competing interest

The authors declare that they have no known competing financial interests or personal relationships that could have appeared to influence the work reported in this paper.

Acknowledgments

This research was supported by grant PID2021-127137-OB-100 funded by MCIN/AEI/10.13039/501100011033 and by "ERDF A way of making Europe". Hiba Salim acknowledges the Generalitat de Catalunya for a FI (Ajuts per a la contractació de personal investigador novell) fellowship. The Bioanalysis group of the UB is part of the INSA-UB Maria de Maeztu Unit of Excellence (Grant CEX2021-001234-M) funded by MICIN/AEI/FEDER, UE. M.V.B. thanks the Canadian Institutes of Health Research grant OV1-170353 for financial support.

Appendix A. Supplementary material

Supplementary data to this article can be found online at https://doi.org/10.1016/j.microc.2024.112505.

Data availability

Data will be made available on reasonable request

References

[1] B. Hu, H. Guo, P. Zhou, Z.L. Shi, Characteristics of SARS-CoV-2 and COVID-19, Nat. Rev. Microbiol. 19 (2021) 141–154, https://doi.org/10.1038/s41579-020-00459-7.
[2] B.D. Kevadiya, J. Machhi, J. Herskovitz, M.D. Oleynikov, W.R. Blomberg, N. Bajwa, D. Soni, S. Das, M. Hasan, M. Patel, A.M. Senan, S. Gorantla, J.E. McMillan, B. Edagwa, R. Eisenberg, C.B. Gurumurthy, S.P.M. Reid, C. Punyadeera, L. Chang, H.E. Gendelman, Diagnostics for SARS-CoV-2 infections, Nat. Mater. 20 (2021) 593–605, https://doi.org/10.1038/s41563-020-00906-z.
[3] P.V. Markov, M. Ghafari, M. Beer, K. Lythgoe, P. Simmonds, N.I. Stilianakis, A. Katzourakis, The evolution of SARS-CoV-2, Nat. Rev. Microbiol. 21 (2023) 361–379, https://doi.org/10.1038/s41579-023-00878-2.
[4] Q. Chen, Z. He, F. Mao, H. Pei, H. Cao, X. Liu, Diagnostic technologies for COVID-19: a review, RSC Adv. 10 (2020) 35257–35264, https://doi.org/10.1039/d0ra06445a.
[5] M. Teymouri, S. Mollazadeh, H. Mortazavi, Z. Naderi Ghale-noie, V. Keyvani, F. Aghababaei, M.R. Hamblin, G. Abbaszadeh-Goudarzi, H. Pourghadamyari, S.M. R. Hashemian, H. Mirzaei, Recent advances and challenges of RT-PCR tests for the diagnosis of COVID-19, Pathol. Res. Pract. 221 (2021) 153443, https://doi.org/10.1016/j.prp.2021.153443.
[6] H. Yang, Z. Rao, Structural biology of SARS-CoV-2 and implications for therapeutic development, Nat. Rev. Microbiol. 19 (2021) 685–700, https://doi.org/10.1038/s41579-021-00630-8.
[7] S. Poolsup, E. Zaripov, N. Hüttmann, Z. Minic, P.V. Artyushenko, I.A. Shchugoreva, F.N. Tomilin, A.S. Kichkailo, M.V. Berezovski, Discovery of DNA aptamers targeting SARS-CoV-2 nucleocapsid protein and protein-binding epitopes for label-free COVID-19 diagnostics, Mol. Ther. Nucleic Acids 31 (2023) 731–743, https://doi.org/10.1016/j.omtn.2023.02.010.
[8] W. Wu, Y. Cheng, H. Zhou, C. Sun, S. Zhang, The SARS-CoV-2 nucleocapsid protein: Its role in the viral life cycle, structure and functions, and use as a potential target in the development of vaccines and diagnostics, Virol. J. 20 (2023) 6, https://doi.org/10.1186/s12985-023-01968-6.
[9] G.K. Uppal, S. Poolsup, E. Zaripov, Y. Gu, M.V. Berezovski, Comparative analysis of aptamers binding to SARS-CoV-2 N protein using capillary electrophoresis and bio-layer interferometry, Anal. Bioanal. Chem. 416 (2024) 1697–1705, https://doi.org/10.1007/s00216-024-05174-3.
[10] A.P. Espejo, Y. Akgun, A.F. Al Mana, Y. Tjendra, N.C. Millan, C. Gomez-Fernandez, C. Cray, Review of current advances in serologic testing for COVID-19, Am. J. Clin. Pathol. 154 (2020) 293–304, https://doi.org/10.1093/AJCP/AQAA112.
[11] M.M. Tantuoyir, N. Rezaei, Serological tests for COVID-19: potential opportunities, Cell Biol. Int. 45 (2021) 740–748, https://doi.org/10.1002/cbin.11516.
[12] A. Ghaffari, R. Meurant, A. Ardakani, COVID-19 serological tests: How well do they actually perform? Diagnostics 10 (2020) 453 https://doi.org/10.3390/diagnostics10070453.
[13] G. Liu, J.F. Rusling, COVID-19 antibody tests and their limitations, ACS Sens. 6 (2021) 593–612, https://doi.org/10.1021/acssensors.0c02621.
[14] R. Pero-Gascon, F. Benavente, Z. Minic, M.V. Berezovski, V. Sanz-Nebot, On-line aptamer affinity solid-phase extraction capillary electrophoresis-mass spectrometry for the analysis of blood α-synuclein, Anal. Chem. 92 (2020) 1525–1533, https://doi.org/10.1021/acs.analchem.9b04802.
[15] H. Salim, L. Pont, E. Giménez, F. Benavente, On-line aptamer affinity solid-phase extraction direct mass spectrometry for the rapid analysis of α-synuclein in blood, Anal. Chim. Acta 1256 (2023) 341149, https://doi.org/10.1016/j.aca.2023.341149.
[16] M. Vergara-Barberán, E.F. Simó-Alfonso, J.M. Herrero-Martínez, F. Benavente, Determination of a lectin protein allergen in food by on-line aptamer affinity solid-phase extraction capillary electrophoresis-mass spectrometry, Microchem. J. 190 (2023) 108746, https://doi.org/10.1016/j.microc.2023.108746.
[17] M. Vergara-Barberán, E.F. Simó-Alfonso, J.M. Herrero-Martínez, F. Benavente, Accurate determination of the milk protein allergen β-lactoglobulin by on-line aptamer affinity solid-phase extraction capillary electrophoresis-mass spectrometry, Talanta 259 (2023) 124542, https://doi.org/10.1016/j.talanta.2023.124542.
[18] L. Pont, R. Pero-Gascon, E. Gimenez, V. Sanz-Nebot, F. Benavente, A critical retrospective and prospective review of designs and materials in in-line solid-phase extraction capillary electrophoresis, Anal. Chim. Acta 1079 (2019) 1–19, https://doi.org/10.1016/j.aca.2019.05.022.
[19] M. Vergara-Barberán, L. Pont, H. Salim, E. Giménez, F. Benavente, On-line aptamer affinity solid-phase extraction capillary electrophoresis-mass spectrometry for the analysis of protein biomarkers in biological fluids and food: a tutorial, Adv. Sample Prep. 7 (2023) 100082, https://doi.org/10.1016/j.sampre.2023.100082.
[20] M. Darmostuk, S. Rimpelova, H. Gbelcova, T. Ruml, Current approaches in SELEX: an update to aptamer selection technology, Biotechnol. Adv. 33 (2015) 1141–1161, https://doi.org/10.1016/j.biotechadv.2015.02.008.
[21] Z. Zhuo, Y. Yu, M. Wang, J. Li, Z. Zhang, J. Liu, X. Wu, A. Lu, G. Zhang, B. Zhang, Recent advances in SELEX technology and aptamer applications in biomedicine, Int. J. Mol. Sci. 18 (2017) 2142, https://doi.org/10.3390/ijms18102142.
[22] V. Pichon, F. Brothier, A. Combès, Aptamer-based-sorbents for sample treatment - a review, Anal. Bioanal. Chem. 407 (2015) 681–698, https://doi.org/10.1007/s00216-014-8129-5.
[23] C. Ge, J. Feng, J. Zhang, K. Hu, D. Wang, L. Zha, X. Hu, R. Li, Aptamer/antibody sandwich method for digital detection of SARS-CoV2 nucleocapsid protein, Talanta 236 (2022) 122847, https://doi.org/10.1016/j.talanta.2021.122847.
[24] S. Ramanathan, S.C.B. Gopinath, Z.H. Ismail, M.K. Md Arshad, P. Poopalan, Aptasensing nucleocapsid protein on nanodiamond assembled gold interdigitated electrodes for impedimetric SARS-CoV-2 infectious disease assessment, Biosens. Bioelectron. 197 (2022) 113735, https://doi.org/10.1016/j.bios.2021.113735.
[25] R. Chen, L. Kan, F. Duan, L. He, M. Wang, J. Cui, Z. Zhang, Z. Zhang, Surface plasmon resonance aptasensor based on niobium carbide MXene quantum dots for nucleocapsid of SARS-CoV-2 detection, Microchim. Acta 188 (2021) 316, https://doi.org/10.1007/s00604-021-04974-z/Published.
[26] R. Pero-Gascon, L. Pont, V. Sanz-Nebot, F. Benavente, On-line immunoaffinity solid-phase extraction capillary electrophoresis-mass spectrometry for the analysis of serum transthyretin, in: T.M. Phillips (Ed.), Clinical Applications of Capillary Electrophoresis, second edition, Humana Press, New York, 2019, pp. 57–76, https://doi.org/10.1007/978-1-4939-9213-3_5.
[27] M.M. Costa, N. Benoit, F. Saby, B. Pradines, S. Granjeaud, L. Almeras, Optimization and standardization of human saliva collection for MALDI-TOF MS, Diagnostics 11 (2021) 1304, https://doi.org/10.3390/diagnostics11081304.
[28] Z. Ghafoori, T. Tehrani, L. Pont, F. Benavente, Separation and characterization of bovine milk proteins by capillary electrophoresis-mass spectrometry, J. Sep. Sci. 45 (2022) 3614–3623, https://doi.org/10.1002/jssc.202200423.
[29] H.H. Lauer, G.P. Rozing, High Performance Capillary Electrophoresis Second Completely Revised Edition A Primer, second edition, Agilent Technologies, Waldbronn, Germany, 2014, pp. 60–63.
[30] ABRF, Association of Biomolecular Resource Facilities, Delta Mass, A database of protein post-translational modifications (2024), https://abrf.org/resources/delta-mass/.
[31] C. Scheller, F. Krebs, R. Minkner, I. Astner, M. Gil-Moles, H. Wätzig, Physicochemical properties of SARS-CoV-2 for drug targeting, virus inactivation and attenuation, vaccine formulation and quality control, Electrophoresis 41 (2020) 1137–1151, https://doi.org/10.1002/elps.202000121.
[32] A. Drees, T.L. Trinh, M. Fischer, The influence of protein charge and molecular weight on the affinity of aptamers, Pharmaceuticals 16 (2023) 457, https://doi.org/10.3390/ph16030457.
[33] A.L. Gassner, S. Rudaz, J. Schappler, Static coatings for the analysis of intact monoclonal antibody drugs by capillary zone electrophoresis, Electrophoresis 34 (2013) 2718–2724, https://doi.org/10.1002/elps.201300070.
[34] M. Biacchi, R. Bhajun, N. Saïd, A. Beck, Y.N. François, E. Leize-Wagner, Analysis of monoclonal antibody by a novel CE-UV/MALDI-MS interface, Electrophoresis 35 (2014) 2986–2995, https://doi.org/10.1002/elps.201400276.
[35] O. Deutsch, Y. Fleissig, B. Zaks, G. Krief, D.J. Aframian, A. Palmon, An approach to remove alpha amylase for proteomic analysis of low abundance biomarkers in

human saliva, Electrophoresis 29 (2008) 4150–4157, https://doi.org/10.1002/elps.200800207.

[36] D. Shan, J.M. Johnson, S.C. Fernandes, H. Suib, S. Hwang, D. Wuelfing, M. Mendes, M. Holdridge, E.M. Burke, K. Beauregard, Y. Zhang, M. Cleary, S. Xu, X. Yao, P. P. Patel, T. Plavina, D.H. Wilson, L. Chang, K.M. Kaiser, J. Nattermann, S. V. Schmidt, E. Latz, K. Hrusovsky, D. Mattoon, A.J. Ball, N-protein presents early in blood, dried blood and saliva during asymptomatic and symptomatic SARS-CoV-2 infection, Nat. Commun. 12 (2021), https://doi.org/10.1038/s41467-021-22072-9.

[37] I. Novodchuk, M. Kayaharman, I. Prassas, A. Soosaipillai, R. Karimi, I. A. Goldthorpe, E. Abdel-Rahman, J. Sanderson, E.P. Diamandis, M. Bajcsy, M. Yavuz, Electronic field effect detection of SARS-CoV-2 N-protein before the onset of symptoms, Biosens. Bioelectron. 210 (2022), https://doi.org/10.1016/j.bios.2022.114331.